ACS APPLIED MATERIALS & INTERFACES

Research Article

www.acsami.org

Robust Superamphiphobic Coatings Based on Silica Particles Bearing Bifunctional Random Copolymers

Ganwei Zhang,[†,‡] Shudong Lin,[†,‡] Ian Wyman,[§] Hailiang Zou,[†,‡] Jiwen Hu,*[,†,‡] Guojun Liu,*[,†,§] Jiandong Wang,[†,§] Fei Li,[†,‡] Feng Liu,[†,‡] and Meilong Hu[†,‡]

[†]Guangzhou Institute of Chemistry, Chinese Academy of Sciences, Guangzhou, People's Republic of China, 510650

[‡]Key Laboratory of Cellulose Lignocellulosics Chemistry, Chinese Academy of Sciences, Guangzhou, People's Republic of China, 510650

[§]Department of Chemistry, Queen's University, 90 Bader Lane, Kingston, Ontario, Canada K7L 3N6

Supporting Information

ABSTRACT: Reported herein is the growth of bifunctional random copolymer chains from silica particles through a "grafting from" approach and the use of these copolymer-bearing particles to fabricate superamphiphobic coatings. The silica particles had a diameter of 90 ± 7 nm and were prepared through a modified Stöber process before atom transfer radical polymerization (ATRP) initiators were introduced onto their surfaces. Bifunctional copolymer chains bearing low-surface-free-energy fluorinated units and sol−gel-forming units were then grafted from these silica particles by surface-initiated ATRP. Perfluorooctyl ethyl acrylate (FOEA) and 3-(triisopropyloxy)silylpropyl methacrylate (IPSMA) were respectively used as fluorinated and sol−gel-forming monomers in this reaction. Hydrolyzing the IPSMA units in the presence of an acid catalyst yielded silica particles that were adorned with silanol-bearing copolymer chains. Coatings were prepared by spraying these hydrolyzed silica particles onto glass and cotton substrates. A series of four different copolymer-functionalized silica particles samples bearing copolymers with similar FOEA molar fractions (f_F) of ~80% but with different copolymer grafting mass ratios (g_m) that ranged between 12.3 wt % and 58.8 wt %, relative to silica, were prepared by varying the polymerization protocols. These copolymer-bearing silica particles with a g_m exceeding 34.1 wt % were used to coat glass and cotton substrates, yielding superamphiphobic surfaces. More importantly, these particulate-based coatings were robust and resistant to solvent extraction and NaOH etching thanks to the self-cross-linking of the copolymer chains and their covalent attachment to the substrates.

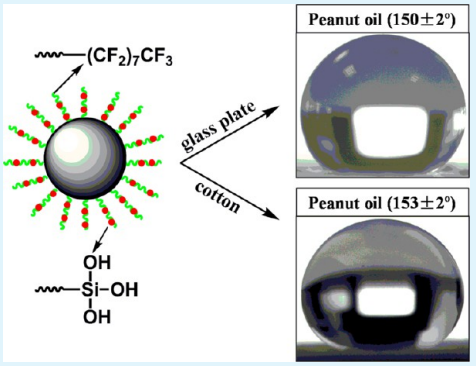

KEYWORDS: *silica particles, superamphiphobic, amphiphobic, surface grafting, coating, sol−gel chemistry, ATRP*

I. INTRODUCTION

Superhydrophobic surfaces exhibit water contact angles of more than 150° and sliding angles of <10°.[1,2] In contrast, amphiphobic or omniphobic surfaces can repel both water and oil, while amphiphobic surfaces exhibiting water and oil contact angles larger than 150° and sliding angles below 10° are considered superamphiphobic.[3−7] Amphiphobic and superamphiphobic coatings have drawn much attention in recent years, because of their applications in many areas, such as self-cleaning surfaces,[3−5,8] water−oil separation,[9] microanalytical instruments,[10] green and nontoxic materials,[11] protection against biological and organic contaminants,[6] sports and outdoor clothing,[12] drag reduction in microfluidic systems,[13] and fingerprint-resistant touch-screen devices.[14]

Many types of superhydrophobic coatings have been inspired by natural surfaces, such as lotus leaves, water strider legs, and butterfly wings.[15,16] Meanwhile, the preparation of superamphiphobic coatings presents a greater challenge, since lipophilic liquids such as cooking oils have a lower surface tension of ~30 mN/m, compared to that for water (~72.1 mN/m). For such a lipophilic liquid to achieve a contact angle of >90° on a flat surface, the coating should have a surface tension of ≤ ~7.5 mN/m.[17,18] Currently, this demand has been met only by fluoroalkyl-bearing surfaces.[19] Unfortunately, these materials are expensive and can have limited effectiveness. Even among fluorinated polymer surfaces, the maximum achievable contact angles on flat coating for water, diiodomethane, and hexadecane droplets with respective surface tensions of 72.1, 50.8, and 27.5 mN/m are only ~120°, ~100°, and ~80°, respectively.[20]

To prepare superamphiphobic coatings, textured surfaces are required that exhibit roughness on both the nanometer and the micrometer scales.[4,5,8,19,21] So far, many methods have been developed to meet this demand for hierarchical roughness in the quest for superamphiphobic coatings. Some of these approaches have included the use of templates,[22,23] lithog-

Received: October 5, 2013
Accepted: November 20, 2013
Published: November 20, 2013

raphy,[24−26] plasma treatment,[19] electrospinning coating techniques,[27−29] and other strategies.[30,31] Among all of these methods, the use of polymers in combination with inorganic particles to fabricate superamphiphobic coatings provides a more straightforward and attractive strategy for developing practical applications. First, fluorinated polymers with low surface energies are easy to prepare, readily tailored, and convenient for large-scale fabrication.[32] In addition, inorganic particles such as silica are also easily prepared.[33] Second, fluorinated polymers are more robust and etchant-resistant than fluorinated small-molecule coupling agents that are frequently used for fabricating superamphiphobic coatings.[34]

Composite materials consisting of fluorinated polymers and inorganic particles can be applied as coatings onto many substrates through traditional coating techniques to render superamphiphobicity.[28,34,35] However, they suffer from two problems. One issue is the poor compatibility between the inorganic particles and the polymers, which may lead to difficult control of the final structures.[36] The other problem is that the coatings had poor stability, since there were no covalent bonds between the inorganic particles, the polymers, and the substrates.

These challenges could be addressed by tuning the polymer compositions and the structures of the coatings, and we have recently made some progress in this area.[17] Toward this end, a new family of bifunctional random copolymers, poly[(perfluorooctylethyl acrylate)-*co*-(tri(isopropyloxy)silylpropyl methacrylate)] or P(FOEA-*co*-IPSMA), were synthesized. Mixtures of these copolymers along with silica particles were used to fabricate superamphiphobic coatings that could be applied onto various substrates through a one-pot process. The particulate coatings were resistant against solvent extraction and NaOH etching because the IPSMA silanol groups underwent condensation reactions among themselves and with the silanol groups on the silica particle surfaces, as well as with the silanol groups on the glass surfaces or hydroxyl groups on cotton fabric or filter paper substrates. However, we found that the copolymer readily filled in the holes and cavities of rough substrates such as filter paper or cotton fabrics, which resulted in a waste of the copolymer. In addition, the silica embedded in the polymer matrix might not have provided coated glass plates with sufficient roughness to impart these surfaces with superamphiphobic properties.[17]

While the P(FOEA-*co*-IPSMA)-based coatings described in our previous report were prepared using blends of copolymers and silica particles, the coatings described in this contribution were based on copolymer-bearing silica particles (Scheme 1).

Scheme 1. Structure of a Polymer-Grafted Silica Particle

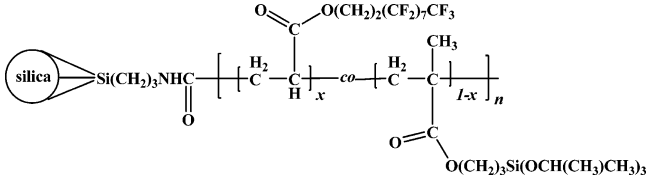

In particular, the P(FOEA-*co*-IPSMA) random copolymers were grown in a "grafting from" manner from silica particles via surface-initiated atom transfer radical polymerization (ATRP). The resultant copolymer-bearing silica particles were subsequently hydrolyzed and then sprayed onto various substrates in order to prepare robust superamphiphobic particulate coatings.

The bifunctional copolymer chains on the silica particles incorporated sol−gel-forming IPSMA units, and thus the hydrolyzed silanol groups of these copolymer chains could co-condense with each other and with the silanol or hydroxyl groups on the substrates. In addition, the FOEA units would migrate to the surface and provide the surface of the coating with a low surface free energy. We envisioned that such a strategy based on these bifunctional silica particles could generate robust superamphiphobic coatings.

To the best of our knowledge, there have been no reports on robust superamphiphobic coatings based on silica particles that were grafted with bifunctional random copolymers that incorporated both fluorinated and cross-linkable units. However, a few approaches have been taken to functionalize silica particles and improve the robustness of superamphiphobic coatings. For example, poly(methacryloxy-propyltrimethoxysilane)-*block*-poly(2,2,3,3,4,4,4-heptafluorobutyl methacrylate)-grafted hybrid silica particles (SiO_2/PMPTS-*b*-PHFBMA) were prepared via a two-step surface-initiated ATRP approach.[36,37] The hybrid particles were used to prepare superhydrophobic surfaces, and the compatibility between the silica particles and the polymers was improved due to the grafting of the polymer chains from the silica particles. Particulate coatings exhibiting tunable surface wetting properties were fabricated from silica particles that were simultaneously coated with a mixture of two diblock copolymers, PIPSMA-*b*-PFOEMA and PIPSMA-*b*-PtBA. Here, PFOEMA and PtBA corresponded to poly(perfluorooctylethyl methacrylate) and poly(*tert*-butyl acrylate), respectively.[38] In another example, stearyl methacrylate-modified polysiloxane bearing pendent epoxy groups was synthesized and coated onto silica surfaces by the "grafting onto" method. These hybrid silica particles were subsequently utilized to fabricate superhydrophobic cotton textiles.[39] Our system differs from the previously studied systems in both the strategy and the polymers used, in that bifunctional random copolymers incorporating both cross-linkable and fluorinated units were grown from the silica particles through a "grafting from" approach. This contribution was undertaken mainly to verify our hypotheses and to develop a simple and practical method for fabricating robust superamphiphobic coatings from bifunctional copolymer-bearing particles.

II. EXPERIMENTAL SECTION

Materials and Reagents. The monomer 2-(perfluorooctyl)ethyl acrylate (FOEA, 97%) was purchased from China Fluoro Technology Co., Ltd., and purified by vacuum distillation over calcium hydride before use. The monomer 3-(tri-2-propoxysiyl) propyl methacrylate (IPSMA) was purchased from Dow Corning Corporation and distilled under reduced pressure prior to use. Methoxyethyl 2-bromoisobutyrate (MEBrIB) was synthesized according to a method described in our previous report, and its structure and purity were confirmed via ^{1}H NMR spectroscopy.[40] Copper bromide (CuBr, Fluka, 98+%) was purified by stirring this reagent in acetic acid at 80 °C for 8 h and washing it more than 10 times with methanol before it was dried overnight under vacuum at room temperature.[41] 4,4′-Dinonyl-2,2′-bipyridined (dNbpy) was purchased from China Nanjing Chemzam Pharmtech Co., Ltd. Tetrahydrofuran (THF) was refluxed with sodium and distilled before use. HCl (4.0 M in dioxane) was purchased from Aldrich and was diluted with THF to a concentration of 0.40 M before use. Triethylamine (Aldrich, 99%) was refluxed with calcium hydride (Aldrich, 97%) overnight and freshly distilled before use. 2-Bromoisobutyryl bromide (Aldrich, 99.0%), (3-aminopropyl)

Table 1. Recipes Used for the Surface-Initiated ATRP of the Comonomers FOEA and IPSMA and Characteristics of the Grafted P(FOEA$_x$-*co*-IPSMA$_{1-x}$)$_n$ Copolymers

run entry/sample name	[FOEA]/[In]	[IPSMA]/[In]	TGA grafting amt, g_m (wt %)	NMR n	NMR x	SEC, M_n (g/mol)	SEC M_w/M_n
1/PS1	20	5	12.3	19	80	4.8×10^3	1.12
2/PS2	32	8	22	33	82	7.4×10^3	1.09
3/PS3	48	12	34.1	49	80		
4/PS4	80	20	58.8	83	81		

triethoxysilane (APTES, Aldrich, 99.0%), tetraethoxysilane (TEOS, Aldrich, 99.0%), α,α,α-trifluorotoluene (TFT, Acros, 99+%), ammonia (Caledon, 28%−30%), copper bromide ($CuBr_2$, Aldrich, 99+%), methanol and absolute ethanol (Aladdin, 99.5%) were used as received. Cotton fabric with an apparent surface density of 13.3 ± 10 mg/cm^2 was purchased from a local factory. A sheet of the cotton fabric was sequentially cleaned by stirring the fabric in a 0.15 wt % detergent solution at 300 rpm for 15 min, washing the fabric via stirring at 300 rpm with 500 mL of distilled water for 15 min for five 15-min cycles, and ultrasonicating the fabric in THF before it was dried at 120 °C in a vacuum oven for 2 h prior to usage. Glass plates (2.4 cm × 2.4 cm) were washed with ethanol thrice and dried at 80 °C in an oven before use.

Silica Particle Preparation. The silica particles were prepared according to a previously reported procedure.[17] Briefly, 300 mL of absolute ethanol and 30 mL of aqueous ammonia solution were mixed together in a 500-mL three-neck round-bottom flask equipped with a condenser. The flask was transferred into a preheated oil bath that was heated at a constant temperature of 60 ± 1 °C. The mixture was homogenized via stirring at 300 rpm for 15 min. Tetraethoxysilane (15 mL) was then added over a period of 30 min and the reaction was allowed to proceed for 24 h. The resultant silica particles were settled via centrifugation at 10 000 *g* for 10 min. After the supernatant had been discarded, the particles were redispersed into 10 mL of absolute ethanol. These particles were settled again via centrifugation and separated from the supernatant by decantation. This rinsing process was repeated thrice. The final particles were dried at 80 °C under vacuum for 24 h to obtain 13.4 g of silica at a yield of 96%. The average diameter of the resulting silica particles evaluated via TEM was 90 ± 7 nm.

Initiator-Functionalized Silica Particles. The silica particles were reacted with APTES in order to functionalize them with amino groups, and these particles were subsequently reacted with 2-bromoisobutyryl bromide.[42,43] In a typical run, 3 g of silica particles were mixed with 60 mL of toluene and 12 mL of anhydrous APTES in a 100-mL flask. After the flask had been subjected to a freeze−pump−thaw treatment and backfilled with argon thrice, it was immersed in an oil bath preheated at 105 ± 1 °C. The mixture was stirred for 24 h before it was washed thrice in sequence with 100 mL of toluene and acetone. The resultant amino-functionalized silica was dried at 50 °C overnight under vacuum to yield 3.1 g of amino-functionalized particles.

A quantity (1.00 g) of the resultant amino-functionalized silica particles was mixed with 50 mL of anhydrous toluene and 15 mL of anhydrous triethylamine in a dried 100-mL flask. The solution was stirred in an ice−water bath for 30 min. Subsequently, 8 mL of 2-bromoisobutyryl bromide and 12 mL of anhydrous toluene were mixed together and slowly added dropwise into the solution over 30 min. After the reaction mixture was stirred for 4 h, it was sequentially washed with excess acetone−water solution (v/v, 1/1), toluene, and acetone before it was precipitated via centrifugation. Initiator-functionalized silica particles (1.04 g) were obtained after they had been dried under vacuum at 50 °C for 24 h.

Preparation of the Polymer-Grafted Silica Particles. The surface-initiated ATRP reaction was performed in a homemade dual-flask system consisting of two 25-mL flasks that were connected via a glass tube with a diameter of 0.8 cm and a length of 5 cm. In a typical run, FOEA (0.6633 g, 1.280 mmol), IPSMA (0.1064 g, 0.320 mmol), TFT (3.5 mL), dNbpy (0.1798 g, or 0.440 mmol), and MEBrIB (0.0045 g, or 0.020 mmol) were added into one of the flasks. Meanwhile, initiator-functionalized silica particles (135 mg, possessing 0.020 mmol of initiating sites), CuBr (28.7 mg, 0.200 mmol), and $CuBr_2$ (4.5 mg, 0.020 mmol) were added into the other flask. The liquid mixture in TFT was bubbled for half an hour before it was subjected to three freeze−pump−thaw cycles, and then carefully transferred to the other flask via the connecting glass tube. The flask containing the resultant brown dispersion was transferred into an oil bath that was preheated at 92 ± 1 °C and this dispersion was stirred for 12 h. The reaction was stopped by freezing the flask with liquid nitrogen before exposing its contents to air, causing the color of the dispersion to change from dark brown to blue. Subsequently, the mixture was centrifuged at 10 000 *g* for 5 min. The free copolymers were collected from the supernatant according to our previously reported method.[17] The precipitated copolymer-functionalized silica particles were redispersed into 5 mL of TFT. These particles were centrifuged again and separated from the supernatant via decantation. This procedure was repeated thrice. Subsequently, the copolymer-functionalized particles were purified further by repeatedly dispersed into 2 mL of anhydrous THF and precipitation from 5 mL of methanol thrice by centrifugation. The final particles were dried overnight under vacuum. The grafting ratio (g_w, wt %), which is denoted as the ratio between the mass of the grafted P(FOEA-*co*-IPSMA) copolymer and that of the silica particles, was ∼22% according to thermogravimetric analysis (TGA), as described in the Results and Discussion section. The process for preparing the above copolymer-grafted silica particles was denoted as run 2, and the resultant silica particles were denoted as PS2 particles. Other functionalized silica particles with different g_w values and denoted as PS1, PS3, and PS4 particles were also prepared via runs 1, 3, and 4, respectively. The preparation protocols for these particles are summarized in Table 1.

Hydrolysis of Copolymer-Functionalized Silica Particles. A sample of copolymer-functionalized silica particles was hydrolyzed under the conditions described in our previous report.[17] In a typical run, 50.0 mg of PS2 was mixed with 30.0 mL of TFT in a 50-mL flask and ultrasonicated for 60 s to disperse the particles. Subsequently, 0.4 mL of THF, 0.4 mL of a HCl solution (0.4 M in THF), and 30.0 μL of H_2O was added in sequence. The mixture was stirred at room temperature for 1 h before it was rinsed in sequence with TFT (3 × 10 mL), THF (3 × 10 mL), and methanol (3 × 10 mL) to remove the catalyst and any byproducts. After they had been centrifuged at 10 000 rpm for 10 min, the hydrolyzed copolymer-functionalized particles were redispersed into TFT at 2.5 mg/mL and used for coating fabrication.

The free copolymer sample of P(FOEA-*co*-IPSMA) that was collected from the supernatant in run 2 was also hydrolyzed under the identical conditions. Samples were collected via syringe at different time intervals and quickly transferred into a centrifuge tube containing a 4-fold volume excess of methanol. The hydrolyzed samples were immediately centrifuged at 10 000 rpm for 5 min, and the resulting precipitates were redispersed into either THF or a mixture of hexafluorobenzene and $CDCl_3$ (v/v = 2/1) for SEC and ^{1}H NMR characterization, respectively.

Amphiphobic and Superamphiphobic Coatings. One milliliter (1 mL) of the hydrolyzed copolymer-functionalized silica particles dispersion at 2.5 mg/mL was spray-coated onto a glass plate (2.4 cm × 2.4 cm) or a piece of cotton fabric (2 cm × 3 cm) using a homemade device.[44] The spray-coating treatment was performed by setting a distance of ∼50 cm between the spinneret (with a diameter of ∼0.1 mm) and the substrate with the aid of nitrogen flow. The coated glass

plate or cotton fabric samples were then dried at 105 °C under vacuum for 2 h.

Coating Durability Tests. To test the robustness of the coated glass plates and the coated cotton samples, they were subjected to solvent extraction as well as NaOH etching tests. In a typical run, the solvent extraction tests were performed by immersing PS3-coated glass plates and cotton fabric samples into a 250-mL beaker filled with 150 mL of TFT, which was stirred with a magnetic bar (cylindrical, $L \times D$ = 3 cm × 0.5 cm) at a speed of 200 rpm for 24 h at room temperature in the presence of these coated samples. Then, the PS3-coated samples were stirred in sequence with THF and methanol for 24 h in every circle. Finally, these coatings were dried under vacuum at 50 °C before the evaluation of their water and oil repellency. Meanwhile, the etching tests were performed by immersing PS3-coated glass plates and cotton fabric samples into a 1.0 M aqueous NaOH solution for various lengths of time (ranging between 1 and 8 h) before the samples were rinsed with water and fully dried under vacuum before peanut oil repellency measurements were performed.

^{1}H NMR and SEC Characterization. All ^{1}H NMR spectra were recorded using a Bruker DMX-400 spectrometer equipped with a Varian probe. A mixture of hexafluorobenzene and $CDCl_3$ (v/v = 2/1) was used as the solvent. Size-exclusion chromatography (SEC) was performed using a Waters 1515 series SEC system equipped with a guard column in addition to styragel HR4, HR3 columns, along with a Waters 2414 refractive index (RI) detector that was set to 35 °C. The columns were calibrated with monodisperse polystyrene standards. The SEC samples were typically prepared at a concentration of 5−10 mg/mL, and they were passed through a 0.45-μm PTFE membrane filter before injection. The mobile phase was high-performance liquid chromatgraphy (HPLC)-grade tetrahydrofuran (THF), which was set to a flow rate of 0.6 mL/min.

Transmission Electron Microscopy (TEM). Transmission electron microscopy (TEM) observations were performed using a JEOL Model JEM-100CXII microscope at an accelerating voltage of 80 kV. Ethanol dispersions of the pristine silica particles or TFT dispersions of copolymer-functionalized silica particles were sprayed onto carbon-coated copper grids using a home-built device[44] and subsequently dried under vacuum at room temperature for 2 h before TEM observation.

Scanning Electron Microscopy (SEM). The substrates and coatings on the substrates were observed by field-emission scanning electron microscopy (SEM) (Hitachi, Model S-4800) after the samples were coated with a thin layer of gold.

Atomic Force Microscopy (AFM). The samples were fixed onto the surface of an atomic force microscopy (AFM) holder, and the surface morphologies of the samples were observed using a Multimode 8 SPM AFM system (Bruker, USA) using a ScanAsyst TM mode.

Thermogravimetric Analysis (TGA). Thermogravimetric analysis (TGA) was performed using a Netzsch Model TGA209F3 instrument. A typical measurement involved heating a sample from room temperature to 850 °C at a rate of 10 °C/min under a nitrogen atmosphere.

Fourier Transform Infrared (FT-IR) Spectra. FT-IR spectra were obtained using a Bruker TENSOR 27 (Germany) instrument operating at a scanning range of 500−4000 cm^{-1}. All samples were dried at ∼80 °C under vacuum for 24 h and then ground with KBr to yield a powder. The spectra were recorded at a resolution of 1 cm^{-1}.

X-ray Photoelectron Spectroscopy (XPS). X-ray Photoelectron Spectroscopy (XPS) (XPS) spectra of the pristine silica particles, the P(FOEA-*co*-IPSMA) copolymer, and PS3 were performed using a KRATOS AXIS Ultra DLD photoelectron spectrometer. A monochromatic Al $K\alpha_{1,2}$ source was used to irradiate a 1-mm-diameter region on each sample at 15 kV, 500−600 W, and 35−40 mA. The pressure in the chamber was kept below 2 × 10^{-8} Torr during the measurements. All binding energy values were calculated relative to the C (1s) photoelectron at 285 eV. The standard takeoff angle used for analysis was 75°, which produced a maximum analysis depth of ∼7 nm.[45]

Contact Angle Measurements. The contact angles of the coated samples were measured using an optical contact angle measuring device (JC2000C, China) at room temperature using 5-μL liquid droplets. The advancing contact angles were measured by slowly injecting 8 μL of the probe liquid into each sample droplet, and the receding contact angles were measured by removing 4 μL of liquid from each sample droplet. For each sample, the contact angles were measured at 5−10 different positions, and the reported values represented the average of these measurements. The liquids used for contact angle measurements were droplets of deionized water, peanut oil (Arawana brand, China), and diiodomethane (>99%, Sigma−Aldrich).

III. RESULTS AND DISCUSSION

Grafting of Silica Particles with Bifunctional Copolymer Chains. The bifunctional copolymer-bearing silica particles were prepared by several steps, as illustrated in Figure 1. The silica particles were initially prepared from tetraethoxysilane via ammonia-catalyzed sol−gel reactions using a modified Stöber procedure.[33] Since the focus of our study was on the grafting of the silica particles with bifunctional copolymer chains to prepare robust superamphiphobic coatings rather than the effect of particle size, only one type of silica particle sample was prepared. The resultant silica particles had an average diameter of 90 ± 7 nm, based on our statistical analysis of more than 200 particles from TEM images.

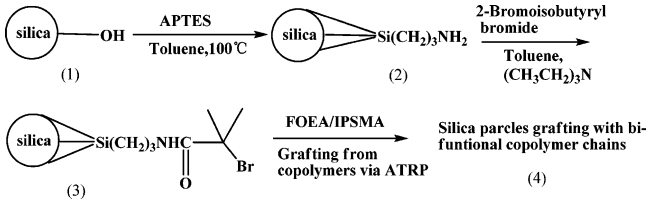

Figure 1. Synthetic route for modifying silica particles and subsequently growing bifunctional copolymer chains from the modified silica particles. Amino group-bearing silica particles were prepared via reaction with APTES (1→2) before an initiator was introduced onto the surfaces of these particles (2→3). Subsequently, bifunctional random copolymer chains were grown from these initiator-bearing particles via ATRP via a "grafting from" approach (3→4).

The initiator-functionalized silica particles were prepared in two steps as shown in Figure 1. The silanol groups (Si−OH) on the surfaces of the silica particles were initially converted into amino groups via reaction with a toluene solution of APTES. These amino-functionalized silica particles were subsequently reacted with 2-bromoisobutyrylbromide to yield 2-bromoisobutyrate-functionalized silica particles. This modification strategy was used to increase the length of the initiator's carbon spacer, which is an important factor for enhancing the grafting densities and initiating efficiencies achieved via surface-initiated ATRP.[46]

The copolymer chains were subsequently grown from the initiator-functionalized silica particles via copper-mediated ATRP of FOEA and IPSMA using dNbpy/CuBr as the catalyst system through a "grafting from" approach. In addition, $CuBr_2$ was added at [CuBr]/[$CuBr_2$] = 10/1 to provide lower polydisperse polymers.[47] A small amount of the free initiator MEBrIB was added to produce some free chains for analysis. Previous studies have indicated that the produced free chains had identical properties as those grafted chains that were produced simultaneously.[48] Since TFT was a good solvent for both PFOEA and PIPSMA, this solvent was used as the

polymerization medium to ensure good control over the polymerization.

In order to study the effect of varying length of the grafted polymer chains, we prepared a total of four P(FOEA-*co*-IPSMA)-functionalized silica samples (PS1−PS4), by changing the monomer-to-initiator ([M]/[In]) ratios in the polymerization protocols, which were otherwise performed under similar polymerization conditions. The polymerization recipes and characteristics of the copolymer-functionalized particles are summarized in Table 1.

FT-IR spectra were recorded to confirm that the bifunctional copolymer chains had been successfully grown from the silica particles. Figure 2 shows the FT-IR spectra of pristine silica particles, 2-bromoisobutyrate-functionalized silica particles, and the PS4 particles. All of the samples exhibited a strong broad peak at ∼1105 cm^{-1} corresponding to the Si−O−Si asymmetric stretching vibration. In addition, peaks at ∼470, ∼800, and ∼940 cm^{-1} corresponding to a Si−O rocking vibration, a Si−O bending vibration, and a Si−O−(H···H_2O) bending vibration, respectively, were also visible. All of these peaks confirmed the formation of silica particles from sol−gel reactions involving tetraethyoxysilane.

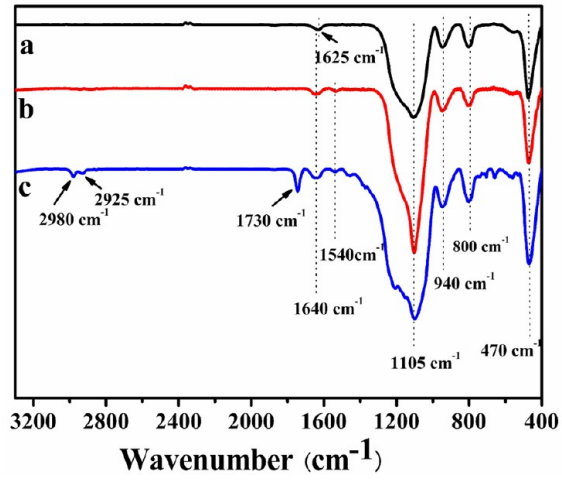

Figure 2. FT-IR spectra of the pristine silica particles (spectrum a), initiator-functionalized silica particles (spectrum b), and PS4 particles (spectrum c).

A new peak at ∼1540 cm^{-1} was visible in Figures 2b and 2c, corresponding to the N−H bending vibration of an amide group. Moreover, the peak at 1625 cm^{-1}, corresponding to the O−H scissoring vibrations of water molecules that had been adsorbed onto pristine silica particles in Figure 2a, was replaced by a peak at 1640 cm^{-1}, which corresponded to the C═O stretching vibrations of amide groups in Figure 2b.[49,50] These obvious differences demonstrated that the 2-bromo-2-methyl-propionyl groups had been successfully attached onto the surfaces of the silica particles.[51] Meanwhile, the peak at 1730 cm^{-1} corresponded to the C═O stretching vibrations of the ester groups from the FOEA and IPSMA units. The absorption bands at 2925 and 2980 cm^{-1}, respectively, corresponded to the $-CH_2$ and $-CH_3$ stretching vibrations of the PFOEA and IPSMA units. In addition, the peak at 1210 cm^{-1} and the series of peaks appearing between 520 and 750 cm^{-1} respectively corresponded to the $-CF_2$ and $-CF_3$ groups of the FOEA units.[52] These spectra thus demonstrated the successful growth of P(FOEA-*co*-IPSMA) chains from the surfaces of the silica particles.

Thermogravimetric analysis (TGA) analysis was also employed to quantify the amount of copolymer that had been grown from the surfaces of the silica particles. Figure 3 shows the TGA traces of pristine silica particles, APTES-modified silica particles, and initiator-functionalized silica particles as well as PS4 and a free chain sample of P(FOEA-*co*-IPSMA) from run 4.

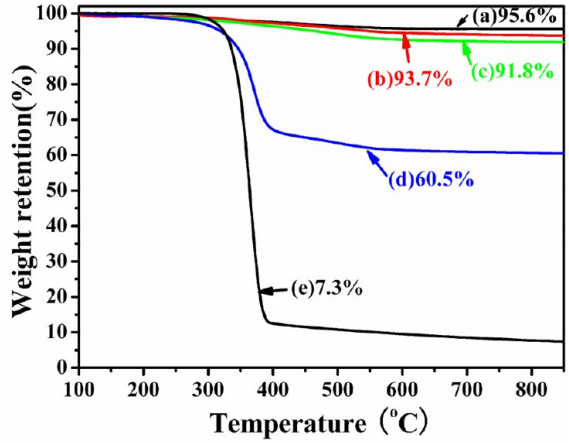

Figure 3. TGA traces of pristine silica (trace a), APTES-modified silica (trace b), 2-bromoisobutyrate-functionalized silica (trace c), PS4 (trace d), and P(FOEA-*co*-IPSMA) from run 4 (trace e).

The traces were all normalized relative to the weights at 100 °C, where adsorbed water would have evaporated under vacuum and no degradation would have occurred at this stage. The residual mass of 95.6% at 850 °C indicated that the silica particles were thermally stable (Figure 3a). Similar profiles with slight changes appeared for both the amino- and initiator-functionalized silica particle samples, which exhibited respective residual masses of 93.7% and 91.8% at 850 °C (see Figures 3b and 3c). Both PS4 and the free copolymer sample from run 4 exhibited a sharp decrease in weight between 300 °C and 400 °C, and they exhibited residual masses of 60.5% and 7.3%, respectively, at 850 °C. The difference of 31.3% in the residual mass between PS4 and that of the initiator-functionalized silica particles can be attributed to the copolymer chains that were attached to the silica particles.

If the residual mass of the amino-functionalized silica particles at 850 °C was used as a reference, one could determine that the initiator-functionalized particles would contain ∼1.48 × 10^{-4} mol of initiator sites per g of functionalized particles. Furthermore, we can roughly estimate the density of ATRP initiators at the surface of the silica particles to be ∼0.37 nm^2/initiator. This value was comparable to ∼0.35 nm^2/initiator on the silica particles with an average diameter of 70 nm reported by Liu et al. using a similar procedure.[53]

As mentioned above, the PS4 particles had a residual mass of ∼60.5% at 850 °C while the sol−gelled P(FOEA-*co*-IPSMA) copolymer sample from run 4 had a residual mass of only 7.3%. If we assumed that the initiator-functionalized silica particles and the sol−gelled P(FOEA-*co*-IPSMA) copolymer were *x* and *y* respectively, and used the residual mass of the initiator-functionalized silica at 850 °C (91.8 wt %) as a reference, we obtained eqs 1 and 2:

$$x + y = 100\% \quad (1)$$

$$91.8\% \times (x + 7.3\%) \times y = 60.5\% \quad (2)$$

Using eqs 1 and 2, we obtained x = 63.0% and y = 37.0%, respectively. Thus, the weight content of the grafted P(FOEA-*co*-IPSMA) relative to that of the silica core, namely, the grafting amount, g_m (wt %), was calculated as ~58.8% for PS4.

Figure 4 shows the TEM images corresponding to the pristine silica particles and the P(FOEA-*co*-IPSMA)-bearing silica particles (PS4). After the P(FOEA-*co*-IPSMA) chains were grown from the particles, a thin copolymer layer was discernible in Figure 4b. In addition, the average diameter of the P(FOEA-*co*-IPSMA)-functionalized silica particles increased from a value of 90 ± 7 nm corresponding to the pristine silica particles to a value of to 103 ± 6 nm, as calculated from the TEM images.

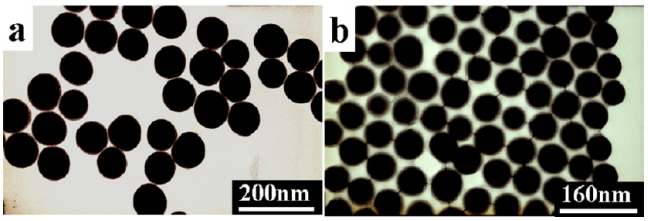

Figure 4. TEM images of (a) the pristine silica particles and (b) the copolymer-bearing silica particles, PS4.

Provided that the density of the grafted polymer including PFOEMA and PIPSMA was 1.91 g/cm^3,[34] the thickness of the grafted polymer layer could be estimated as 8 nm. Therefore, the diameter of the polymer-grafted silica particles should be ~106 nm, which is comparable with the average value calculated from the TEM images. It should be mentioned that stripes were observed between these polymer-grafted silica particles in the TEM image shown in Figure 4b, which may have been due to damage by the electron beam during TEM analysis.[54]

Evidently, the grafting amount of P(FOEA-*co*-IPSMA) (expressed as the weight of the copolymer with respect to the weight of the silica particles) increased with increases of [FOEA]/[In] and [IPSMA]/[In]. To shed light on the characteristics of the P(FOEA-*co*-IPSMA) copolymers that grew from the silica particles, we investigated samples of the free copolymer that were derived from the corresponding run. It has been reported that the polymer chains that were grown from free initiators had molecular weights identical to those that were grown from initiator-functionalized particles.[48] Therefore, the samples of P(FOEA-*co*-IPSMA) prepared from corresponding runs were used as models for the covalently bound copolymers and characterized via SEC using THF as the eluent. SEC traces of only two of these copolymers were recorded as listed in Table 1, because the samples with high g_m values had poor solubility in THF. Low M_w/M_n values of 1.12 and 1.09 were observed for the P(FOEA-*co*-IPSMA) copolymer samples, corresponding to those that were bound to PS1 and PS2, respectively, suggesting that the ATRP reaction proceeded in a controlled fashion.[48]

The free copolymer samples from runs 1−4 were also characterized via ^{1}H NMR spectroscopy, using a mixture of hexafluorobenzene and $CDCl_3$ (v/v = 2/1) as the solvent. Their x and n values were calculated according to the method described in our previous report,[17] and the results are shown in Table 1. The M_w value of the grafted P(FOEA-*co*-IPSMA) sample was calculated as 9.1 × 10^3 g/mol for PS1. Thus, the grafting density of P(FOEA-*co*-IPSMA) chains on the surface of the silica particles was estimated as ~4.1 chains/nm^2 and the initiator efficiency of the surface-initiated ATRP leading to the PS1 particles was ~9.0%. The initiator efficiency for PS2, PS3, and PS4 was calculated as 9.3%, 9.7%, and 9.8%, respectively. The relatively low initiator efficiencies may have resulted from the bulkiness of the FOEA units.[53,55] This was also consistent with the findings of other researchers who had grafted various polymers onto silica particles.[56]

Hydrolysis of the Copolymer-Bearing Silica Particles. The copolymer-bearing silica particles were hydrolyzed in a TFT/THF mixture using HCl as a catalyst. This process involved the hydrolysis of IPSMA to yield silanol groups, which subsequently underwent condensation among themselves. The hydrolysis and the condensation of these silanol groups were influenced by the reaction temperature, the sample concentration, and the amount of catalyst.[57−59] In order to covalently bind functional silica particles onto the substrate to prepare superamphiphobic coatings, we used a trace amount of HCl to catalyze the IPSMA hydrolysis and prevent the particles from

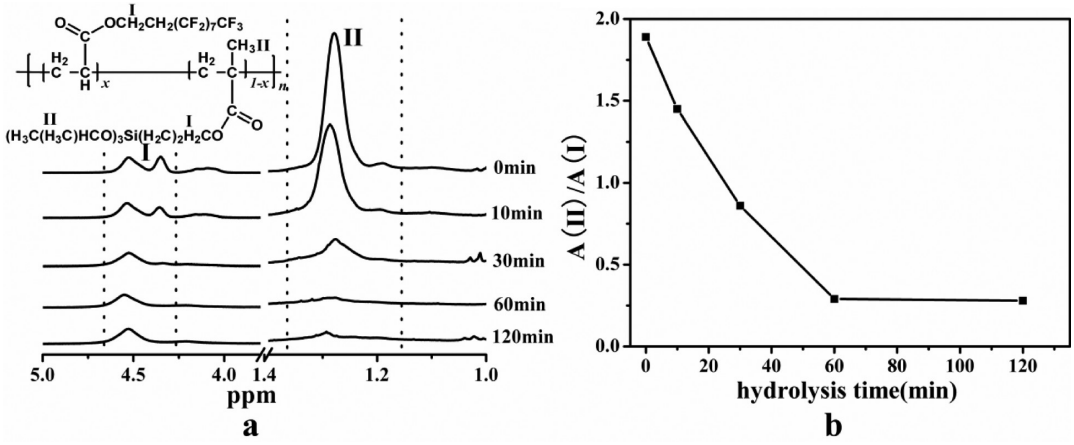

Figure 5. (a) ^{1}H NMR spectra of P(FOEA-*co*-IPSMA) recorded in a mixture of hexafluorobenzene and $CDCl_3$ at v/v = 2/1. (b) Changes in A(II)/A(I) with the hydrolysis time, as derived from the ^{1}H NMR spectra.

undergoing condensation in solution before they were applied onto the substrate.

The hydrolysis process was monitored by SEC and ^{1}H NMR measurements using P(FOEA-*co*-IPSMA) samples instead of copolymer-functionalized silica particles. Figure 5a shows the variation of the ^{1}H NMR spectra of copolymers prepared via run 2 during the hydrolysis process. Visually, the integration (A(II)) of the signal at 1.28 ppm (labeled as "II" in Figure 5a) corresponding to the methyl groups of PIPSMA decreased dramatically with the hydrolysis time. To obtain quantitative results, the integration (A(I)) of signals in the range between 4.25 ppm and 5.75 ppm of (labeled as "I" in Figure 5a) was used as a reference, and we thus plotted the variation of the A(II)/A(I) ratio with the hydrolysis time, as shown in Figure 5b.

This ratio decreased from ~1.85 to ~0.28 during the first hour and then leveled off as the reaction proceeded further. The stabilized value of 0.28 was very close to the theoretical value of 0.27 that would be anticipated for a fully hydrolyzed sample after the $-CH_3(CH_3)-$ signal disappeared, thus implying that the IPSMA units underwent a complete hydrolysis within 1 h under these conditions.

The molecular weights (M_n) and retention times of samples that were collected at various stages during the hydrolysis reaction were also recorded via SEC. Samples that had been hydrolyzed for 0, 10, 30, 60, and 120 min had M_n values of 7.4 × 10^3, 7.6 × 10^3, 7.6 × 10^3, 7.1 × 10^3, and 7.4 × 10^3 g/mol, respectively. The retention time did not change significantly and remained at ~15 min. These results suggested that the copolymers did not undergo condensation within 2 h. Therefore, the copolymer-functionalized silica particles were completely hydrolyzed, but did not undergo condensation in the time period ranging between 1 and 2 h, and thus could provide robust amphiphobic or superamphiphobic coatings.

Amphiphobic or Superamphiphobic Coatings. Glass plates were spray-coated with various hydrolyzed copolymer-bearing silica particles. The coated glass plates were subsequently vacuum-dried at 105 °C for 2 h to stabilize the coatings. During this procedure, the hydrolyzed IPSMA units underwent condensation reactions with each other and with the silanol groups on the glass substrate, thus yielding Si−O−Si bonds between these particles and with the substrate.[17] A proposed structure of this coating is shown in Figure 6.

The current strategy for fabricating superamphiphobic coatings utilizes silica particles that were grafted with bifunctional copolymers (Figure 6). We envisioned that the FOEA units could migrate to the surface of the coating due to the low surface tension of the fluoroalkyl groups. This hypothesis was verified via X-ray photoelectron spectroscopy (XPS), as described in our previous report.[17] Figure 7 shows the XPS spectra of pristine silica particles, the P(FOEA-*co*-IPSMA) copolymer prepared from run 4, PS4 particles, and a hydrolyzed PS4-based coating covering a glass plate.

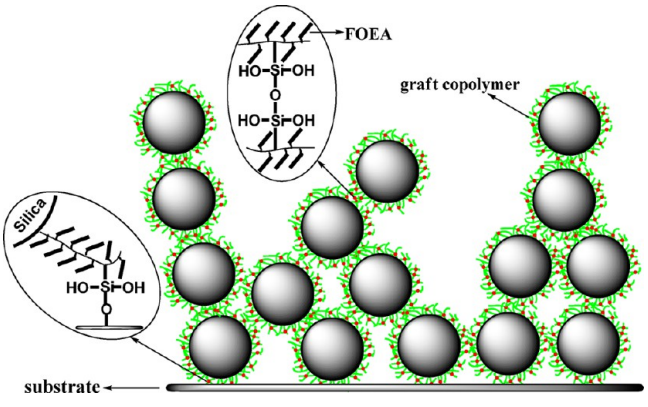

Figure 6. Proposed structure of the particulate coating prepared from hydrolyzed P(FOEA-*co*-IPSMA)-functionalized silica particles.

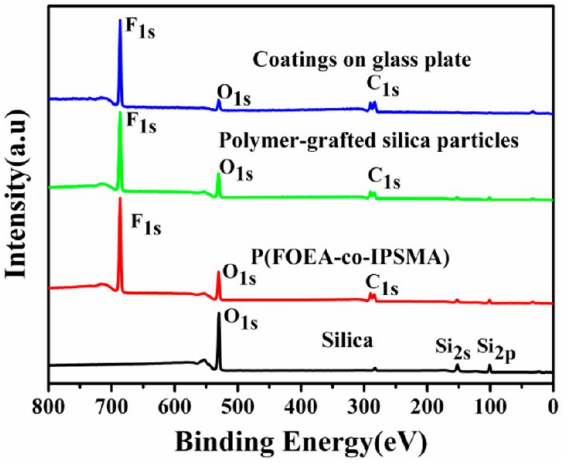

Figure 7. XPS spectra of the pristine silica particles, P(FOEA-*co*-IPSMA) from run 4, polymer-functionalized silica particles (PS4), and of a PS4-based coating covering a glass plate (shown as black, red, green, and blue spectra, respectively).

A weak C 1s peak was observed at 284 eV in the XPS spectrum of the pristine silica particles, which may be attributed to an incomplete hydrolysis of the alkoxide precursor or to organic contaminants.[60] The pristine silica particles mainly exhibited Si signals (~150 eV for Si 2s and ~100 eV for Si 2p) and O (~535 eV for O 1s). Meanwhile, the P(FOEA-*co*-IPSMA) copolymer produced from run 4 and the PS4 particles exhibited F (~690 eV for F 1s and ~30 eV for F 2s), and C (complex peaks at 280−295 eV for C 1s) signals, as expected, in addition to similar Si and O signals as displayed by the silica particles. A similar XPS profile displaying F, O, C, and Si signals was also exhibited by the PS4-based coating covering the glass plate.

The atomic ratio between F, C, O and Si ($N_F/N_C/N_O/N_{Si}$) was also estimated from the XPS survey spectra of the corresponding samples. Both this value calculated from the XPS spectra, and the theoretical values calculated from the chemical structure are listed in Table 2. The fluoride content, as estimated from the XPS spectra, was higher than the theoretical

Table 2. Atomic Ratios of F, C, O, and Si ($N_F/N_C/N_O/N_{Si}$) at the Surfaces of Various Samples as Estimated from the XPS Spectra and from the Chemical Formula

sample	structural ratio $N_F/N_C/N_O/N_{Si}$ (%) ratio[a]	experimental $N_F/N_C/N_O/N_{Si}$ (%) ratio[b]
copolymer from run 4	44.2/46.8/8.4/0.6	55.7/37.8/5.9/0.6
PS4	44.2/46.8/8.4/0.6	57.2/26.9/11/4.9
PS4 coating	47.2/43.8/8.3/0.7	62.4/31.8/5.1/0.7

[a]Value calculated from the structure. [b]value estimated from the XPS spectra.

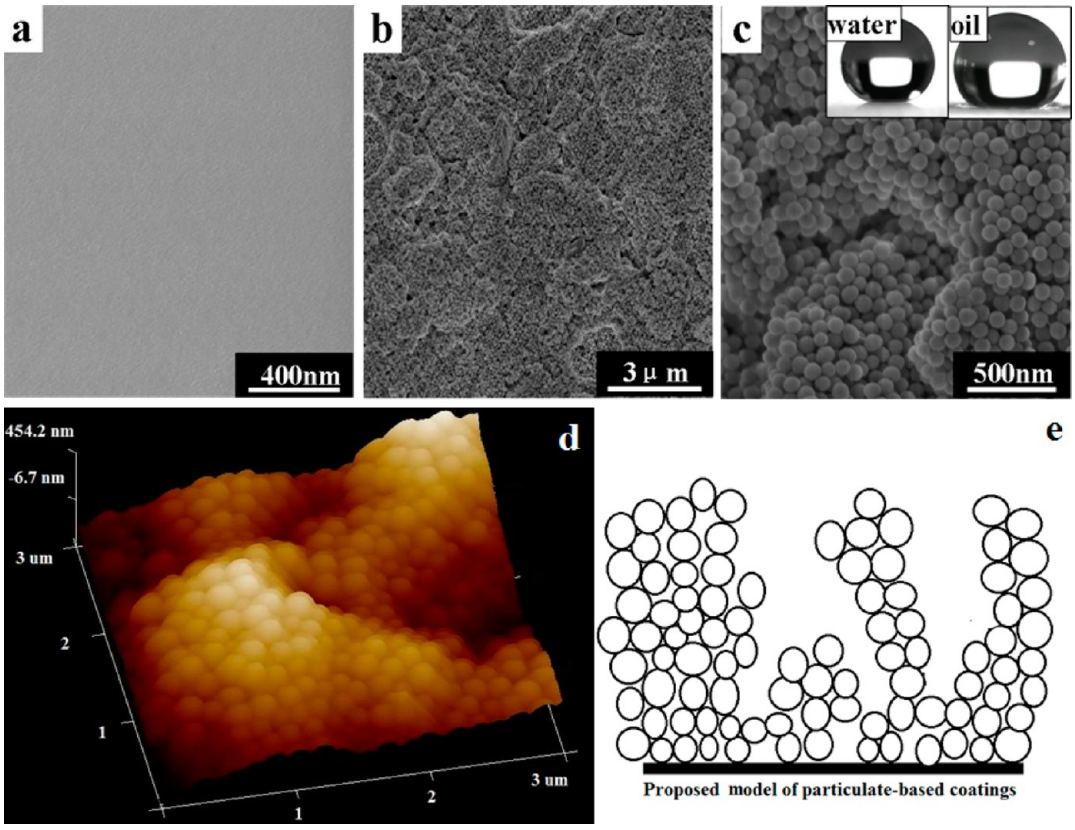

Figure 8. SEM images of (a) a glass plate and (b and c) a PS3-coated glass plate. The insets in panel c are photographs of water and peanut oil droplets sitting on the resulting coated glass plate, respectively. Also shown are (d) a three-dimensional (3D) topography image of a PS3-coated glass plate and (e) a schematic illustration showing the proposed structure of the particle-based coating.

value calculated from the corresponding chemical structure, indicating that the surfaces of the films were enriched with fluorinated domains. This surface enrichment of fluorine-based species bearing a highly bilayered structure was due to the vertical alignment of neighboring perfluoroalkyl groups, which is a well-known phenomenon among PFOEA films bearing long perfluoroalkyl chains.[45] This behavior results from the tendency of the PFOEA films to minimize their overall free energy by allowing low-energy constituents to enrich the surface.

The coatings prepared from the PS4 particles had the highest fluoride content within this series, implying that the highest degree of bilayer structure was obtained if the coating was subsequently annealed at 105 °C, which was well above PFOEA's glass-transition temperature of 52 °C.[61] This annealing treatment would likely facilitate rearrangement within the film, thus allowing the fluorinated units to migrate to the surface and lower the surface energy. It should be mentioned that since the hydroxyl group is highly hydrophilic, it was somewhat surprising that the prepared coating exhibited amphiphobic or even superhydrophobic behavior. This behavior further suggested that the hydroxyl groups were embedded beneath the surfaces of the coatings, which were enriched with fluorine-based species. The fluorinated species would exhibit a highly bilayered structure due to the vertical alignment of neighboring perfluoroalkyl groups.

It was mentioned above that water and oil repellency are not only dependent on the low surface energy of a coating, but also on the surface roughness. Therefore, the structures of the coatings prepared from the copolymer-functionalized silica particles were observed via SEM. Figure 8 shows the morphologies of an uncoated glass plate and a PS3-coated glass plate that was recorded at various magnifications. While the uncoated glass plate was relatively smooth (Figure 8a), the PS3-coated glass plate was fully covered by the particulate coating, as indicated by the SEM image that was recorded at a lower magnification and shown in Figure 8b.

Meanwhile, the higher magnification SEM image shown in Figure 8c revealed that the polymer-grafted silica nanoparticles were clearly visible, with an average diameter of ∼100 nm. This diameter was consistent with that of their precursors, P(FOEA-*co*-IPSMA)-bearing silica particles that were observed via TEM (recall Figure 4b). Nevertheless, these particles were not uniformly clustered together, so they thus formed "islands". The diameters of some of these "islands" were in the micrometer scale, thus demonstrating that the coating exhibited multiscale roughness. Since the same coating method was used, we observed similar structures among glass plates that were coated with the other three polymer-grafted silica particle samples.

The surface topography of the PS3-based particulate coating was further investigated by AFM (Figure 8d). The surface coverage observed via AFM image was consistent with that observed from the SEM images shown in Figure 8c. The images also demonstrated that nanoparticles had a tendency to aggregate together to form clusters. That is, the particles formed random agglomerates with fractal island-like growth behavior, as clearly evidenced by the "hill-to-valley" surface cavities created from aggregated nanoparticles. Such cavities typically extended at least ∼200−600 nm into the film, as

Table 3. Static, Advancing, and Receding Contact Angles of Water, Diiodomethane, and Peanut Oil Droplets on Glass Plates Coated with Various Copolymer-Functionalized Silica Particles

	Water			Diiodomethane			Peanut Oil		
coating particles	θ_s (°)[a]	θ_a (°)[b]	θ_r (°)[c]	θ_s (°)[a]	θ_a (°)[b]	θ_r (°)[c]	θ_s (°)[a]	θ_a (°)[b]	θ_r (°)[c]
PS1	140 ± 2	145 ± 2	134 ± 2	135 ± 2	137 ± 2	124 ± 2	121 ± 2	126 ± 2	113 ± 2
PS2	152 ± 2	154 ± 2	147 ± 2	148 ± 2	150 ± 2	139 ± 2	136 ± 2	139 ± 2	126 ± 2
PS3	159 ± 2	161 ± 2	154 ± 2	155 ± 2	157 ± 2	150 ± 2	150 ± 2	152 ± 2	143 ± 2
PS4	160 ± 2	162 ± 2	156 ± 2	156 ± 2	158 ± 2	152 ± 2	151 ± 2	153 ± 2	145 ± 2

[a]Static contact angle. [b]Advancing contact angle. [c]Receding contact angle.

revealed by the cross-section thickness traces (the height difference between the highest and lowest pixels; see Figure S1 in the Supporting Information). In addition, the surface roughness (rms) of this particulate film was ~140 nm. Figure 8e shows an illustration of a proposed model of a particle-based coating consisting of individual particles as well as clusters of particles and thus exhibits "hill-to-valley" surface cavities. This model was proposed based on the AFM and SEM observations mentioned above (see Figures 8c and 8d).

The inset in Figure 8c shows photographs of water and peanut oil droplets that were placed on PS3-coated glass plates. The water and oil repellency were evaluated by measuring the static water/oil contact angles and the corresponding hysteresis angles (difference between the advancing and receding contact angles). The PS3-coated glass plates had a static water contact angle of 159° ± 2° and a hysteresis angle of 7° ± 2°, a static diiodomethane contact angle of 155° ± 2° and a hysteresis angle of 7° ± 2°, as well as a static peanut oil contact angle of 150° ± 2° and a hysteresis of 9° ± 2° (Table 3).

Since the static contact angles were larger than 150° and the hysteresis was less than 10°, the PS3-coated glass plate was believed to be superamphiphobic.[1,2] It should be mentioned that while the water and diiodomethane droplets rolled readily off the PS3-coated glass plate, the peanut oil droplets did not roll as cleanly as the water and diiodomethane droplets and left residues after the majority of a droplet had rolled off.

Glass plates were also coated with the other three copolymer-functionalized silica particle samples (PS1, PS2, and PS4) under similar conditions. The water, diiodomethane, and oil repellencies of these coated glass plates were also evaluated, and they are summarized in Table 3. The PS1-coated glass plate had a water contact angle of 140° ± 2° with a hysteresis of ~11°, a diiodomethane contact angle of 135° ± 2° with a hysteresis of ~13°, as well as a peanut oil contact angle of 121° ± 2° with a hysteresis of ~13°. These relatively modest values were believed to be due to the fact that the surfaces of the PS1 particles were not fully covered by copolymer chains, as suggested by their low grafting ratio. Meanwhile, the PS2-based coatings exhibited a water contact angle exceeding 150° with a hysteresis of less than 10°, a diiodomethane contact angle of 148° ± 2° with a hysteresis of ~11°, and a peanut oil contact angle of 136° ± 2° with a hysteresis of ~13°. While water droplets could readily roll off the PS2-coated glass plate, the diiodomethane and oil droplets did not roll off freely but remained on the surface. This demonstrated that coatings derived from PS2 were superhydrophobic rather than superamphiphobic.[1,2] However, compared to PS3-coated glass plates, the superamphiphobicity was slightly improved, as judged by the fact that the PS4-coated glass plate had a static water contact angle of 160° ± 2° with a hysteresis angle of 6° ± 2°, a static diiodomethane contact angle of 156° ± 2° with a hysteresis angle of 6° ± 2°, as well as a static peanut oil contact angle of 151° ± 2° with a hysteresis of 8° ± 2° (see Table 3). Moreover, in this case, the water, diiodomethane and the peanut oil droplets all rolled readily off the PS4-coated glass plates. These demonstrated that both the water and oil repellency could be adjusted by changing the copolymer grafting ratio (g_m).

Compared to the amphiphobic glass plate prepared by using blends of copolymers and silica particles as described in our previous report, the glass plates that were coated using the current strategy were rendered superamphiphobic.[17] We believed that the rough texture of the coating is the key factor that induced such repellency difference for both coatings. The SEM characterization of the coated glass plates prepared by using blends of copolymers and silica particles revealed that they exhibited roughness on the nanoscale, but not the microscale. On this basis, it could be anticipated that their self-cleaning properties would be limited, as reflected by their contact angles that were in the amphiphobic regime, but fell short of the superamphiphobic regime.[17] On the contrary, glass plates that were coated using the current strategy were rendered superamphiphobic and exhibited roughness on not only the nanoscale, but also the microscale.

Two distinct models by Wenzel[62] and Cassie–Baxter[63] were frequently employed to explain the effect of roughness on the wetting behavior. In Wenzel's model, the actual surface area is effectively increased with roughness. The apparent Wenzel contact angle (θ^w) on a rough surface can be expressed by eq 3:

$$\cos \theta^w = r \cos \theta_0 \tag{3}$$

where r is the roughness factor and is defined as the ratio of actual surface area over the apparent surface area. Meanwhile, θ_0 denotes the equilibrium contact angle on a homogeneous surface or the Young's contact angle. In the Cassie–Baxter model, the apparent contact angle (θ^c) on a heterogeneous surface can be described by eq 4:

$$\cos \theta^c = f_1 \cos \theta_1 + f_2 \cos \theta_2 \tag{4}$$

where f_1 and f_2 are fractions of different surface components ($f_1 + f_2 = 1$), while θ_1 and θ_2 correspond to the Young's contact on the homogeneous surface of each respective component. When air is trapped in the grooves of a rough surface, the surface is considered to be a composite surface consisting of both solid and air, and θ_2 in air is equal to 180°. The Cassie–Baxter model can thus be rewritten as eq 5:

$$\cos \theta^c = f_1(\cos \theta_1 + 1) - 1 \tag{5}$$

where f_1 denotes the fraction of liquid–solid contact. θ^c increases with the decrease of f_1 when more air is trapped between the grooves of the rough surface.

Since the roughness factor (r) was 1.35, as estimated from the AFM data analysis software, the theoretical Wenzel water

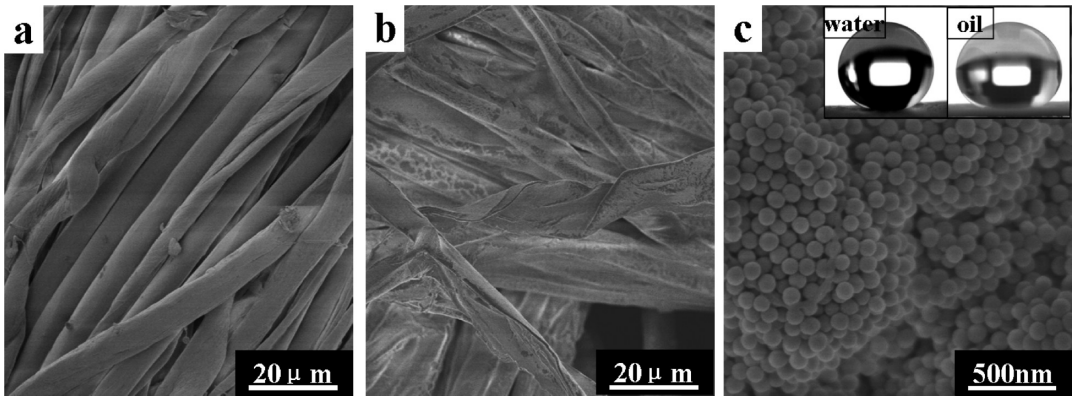

Figure 9. SEM images of the uncoated (a) and PS3-coated (b) cotton fabrics. Image (c) shows a magnified view of an individual PS3-coated cotton fiber, while the inset images shown are photographs of water and peanut oil droplets sitting on a PS3-coated cotton fabric.

contact angle (θ^w) can be estimated to be ~123°. The measured contact angle for the PS3 particle based coating was ~159°, which was much higher than the predicted Wenzel contact angle. This suggested that water did not penetrate grooves between the aggregates of particles. Consequently, the surface of the PS3 particle-based coating could be considered as a Cassie–Baxter nonwettable surface with air pockets trapped between the aggregates of particles.[64]

The fraction of liquid–solid contact, denoted as f_1 in the Cassie–Baxter model, was calculated to be ~0.16, based on the sum of the lengths of the lines between the individual peaks over the length of entire lines (see Figure S1 in Supporting Information). Here, more than 20 cross-sectional data plots were used to evaluate f_1. Since the θ_1 value was ~114° for a flat PFOEA surface casted from PFOEA solution in 1,1,2-trichlorotrifluoroethane,[45] the calculated contact angle from the Cassie–Baxter model was 155°, which was comparable to the observed water contact angle of 159° for the PS3 particle-based coating. This confirmed that PS3 nanoparticles had a tendency to become agglomerated together to form "island" clusters. These clusters provided a rough morphology, and this higher surface roughness allowed a large amount of air to become entrapped to reduce the contact area between the liquid droplets and the surface. Therefore, the effects of both the roughness and the low-surface-energy fluorinated units provided the coatings with superamphiphobicity.

Previously, we have found that cotton textiles provided ideal substrates for fabricating superamphiphobic coatings,[17,58] since the roughness was enhanced by micrometer-sized cotton fibers. Therefore, we anticipated that coating cotton textiles with these copolymer-functionalized nanoparticles would further promote the superamphiphobicity, by exhibiting both nanoscale and microscale roughness.

PS3 particles were dispersed into TFT and hydrolyzed before they were sprayed onto cotton fabrics using identical conditions to those used to coat the glass plates. Figure 9 shows SEM images of the unmodified cotton fabric and coated cotton fabric. The fibers of the unmodified cotton fabric had an average diameter of 9 ± 3 μm and were clearly visible in Figure 9a. The fibers of the coated cotton were covered by a relatively uniform coating, as can be seen in the SEM image shown in Figure 9b. More importantly, the individual fibers were clearly visible, indicating that their structure was retained along with the fabric's microscale roughness. Figure 9c shows a high-magnification SEM image of an individual PS3-coated cotton fiber, in which the PS3 particles were clearly visible and uniformly packed.

Photographs of water and peanut oil droplets sitting on PS3-coated cotton fabrics are shown in the inset of Figure 9c. While the original cotton fabric was hydrophilic, the PS3-coated fabric was superamphiphobic, as demonstrated by the fact that the water/oil static contact angles exceeded 150° and the corresponding hysteresis angles were less than 10°. For example, static water contact angles, advancing and receding contact angles were 163° ± 2°, 164° ± 2°, and 161° ± 2°, respectively. The peanut oil contact angles were 153° ± 2°, 155° ± 2°, and 147° ± 2°, respectively. Meanwhile, the diiodomethane contact angles were 157° ± 2°, 159° ± 2°, and 154 ± 2°, respectively. Again, the superhydrophobicity of PS3-coated cotton fabrics prepared using the current strategy was slightly improved compared to that of the coatings prepared using the strategy reported in our previous paper.[17]

It should also be noted that we have provided both glass plates and cotton textiles with superamphiphobic properties. In comparison, we have previously provided glass plates and cotton textiles with amphiphobic and superamphiphobic properties, respectively, using a blend of silica particles and random copolymers to prepare the coatings.[17] In addition, the particles described in this report require a copolymer grafting ratio of only 34.1 wt %, relative to the silica particles, as opposed to a grafting ratio of ~150% to render similar amphiphobicity or superamphiphobicity in the previous report.[17] This suggested that our current strategy of growing the copolymer chains from the silica particles through a "grafting from" approach provided more-efficient building blocks for self-cleaning coatings.

Robustness of the Superamphiphobic Coatings. According to the formation mechanism for the superamphiphobic coatings shown in Figure 6, it was proposed that the copolymer-functionalized silica particles formed covalent bonds with each other and with the substrate. This covalently bound structure would endow the coatings with the stability required for various applications. Solvent extraction tests were thus performed to demonstrate the robustness of these coatings. The PS3-coated glass plate and cotton samples did not exhibit any significant changes in their water and peanut oil static contact angles after they were subjected to the solvent extraction tests, which involved stirring the coated samples initially in TFT, before they were stirred in THF, and then methanol for 24-h cycles. In addition, they also exhibited very little change in their advancing and receding contact angles,

which thus demonstrated that these coatings were robust against solvent extraction. For comparison, glass and cotton substrates were coated with the copolymer-functionalized silica particle dispersions under otherwise similar conditions except that no hydrolysis treatment was performed. In the absence of hydrolysis treatment, the coatings were easily rinsed away from both of these substrates during the solvent extraction tests, thus demonstrating the importance of this step for achieving robust coatings. These durability tests demonstrated that the polymer-functionalized silica particles provided stable coatings that withstood solvent extraction, because of the fact that these particles were chemically bound to each other and to the substrate.

The robustness of these coatings was further demonstrated by their resistance against etching by NaOH. Figure 10 shows

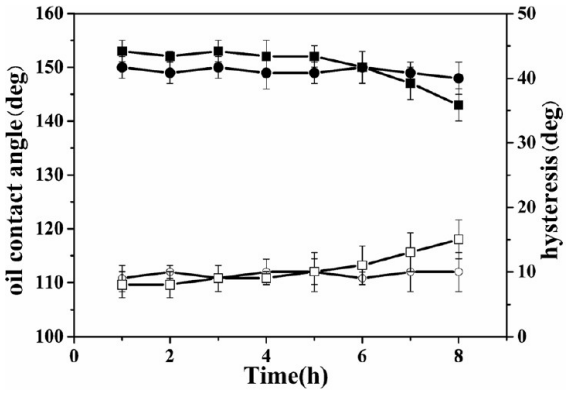

Figure 10. Variation of the peanut oil contact angles and hysteresis angles as functions of the soaking time in a 1.0 M NaOH solution. Shown are (●) peanut oil contact angles and (○) hysteresis angles measured on PS3-coated glass plates, as well as (■) peanut oil contact angles and (□) hysteresis angles measured on PS3-coated cotton fabrics.

the dependence of the peanut oil contact angles and the hysteresis on the soaking time. The contact angles and hysteresis of the PS3-coated glass plates did not change significantly after they had been soaked in 1.0 M NaOH solution for 8 h. Meanwhile, the PS3-coated coated cotton fabrics exhibited a decrease in their contact angles from 153° to 143°, while their hysteresis increased gradually from ∼8° to ∼15° as their immersion time in NaOH solution was increased from 1 h to 8 h. This diminished performance might be due to a rougher and relatively loose structure of the coating covering the cotton fabrics, so that the coating may be more prone to etching by NaOH than the relatively compact coatings covering the glass plates.

Because we do not have access to a suitable testing facility, we have not formally evaluated the wear resistance of our coatings. Despite this, our preliminary evaluation suggests that coatings prepared through our current approach have similar mechanical robustness as that exhibited by the coatings prepared using blends of the P(FOEA-*co*-IPSMA) and silica particles, which was described in our previous report.[17] Moreover, the coatings from our current approach appear to have greater mechanically durability than those prepared from silica particles that were coated with PIPSMA-*b*-PFOEMA. For example, while particulate coatings based on PIPSMA-*b*-PFOEMA-covered silica particles were readily removed by swiping them with a finger,[34] the coatings prepared through the currently reported approach remained firmly bound to the filter paper and could not be swiped off with a finger.

IV. CONCLUSION

We have developed a novel strategy for fabricating superamphiphobic coatings from silica particles that were adorned with bifunctional random copolymers. This strategy utilized a "grafting from" approach, in which the random copolymers were grown from the silica particles via atom transfer radical polymerization (ATRP). A series of four different P(FOEA-*co*-IPSMA)-bearing silica particles were synthesized and characterized, and they exhibited grafting ratios (g_m) ranging between 12.3 wt % and 58.8 wt %, according to thermogravimetric analysis (TGA) analysis. The surface-initiated ATRP was conducted in a controllable manner through the use of a free initiator. After hydrolysis, the copolymer-functionalized silica particles were spray-coated onto glass plates and cotton fabrics. These particle-based coatings provided glass plates with superamphiphobic properties, provided that g_m was more than 34.1 wt %. Moreover, these coatings provided cotton fabrics with further improved superamphiphobic properties due to their roughness enhanced by micrometer-sized cotton fibers and also due to the low surface free energy provided by the copolymer's FOEA units. The particulate coatings were robust and resistant to both solvent extraction and NaOH etching because the copolymer-functionalized silica particles were covalently bound with each other and to the substrates. These functional particles should be useful for fabricating robust superamphiphobic coatings that can be applied onto a wide range of hydroxyl-group bearing substrates, such as glass, cotton, wood, and numerous other substrates.

■ ASSOCIATED CONTENT

Ⓢ Supporting Information

Supporting Information, including an AFM height image of a PS3-coated glass plate, and AFM cross sections of the line shown in the height image are also available. This material is available free of charge via the Internet at http://pubs.acs.org.

■ AUTHOR INFORMATION

Corresponding Author

*E-mail: hjw@gic.ac.cn.

Notes

The authors declare no competing financial interest.

■ ACKNOWLEDGMENTS

We thank the National Natural Science Foundation of China (Nos. 20474068 and 51173204), the Leading Talents Program of Guangdong Province, Guangzhou Invited-Talents Special Project for Addressing Challenging Problems (No. 11D34060038), and Guangzhou Science and Technology Tackling Fund (No. 11A24060596) for providing financial support. G.L. wishes to thank NSERC of Canada for funding and for a Tier 1 Canada Research Chair Position in Materials Science.

■ REFERENCES

(1) Wang, S.; Jiang, L. *Adv. Mater.* **2007**, *19*, 3423−3424.
(2) Wang, H. X.; Ding, J.; Xue, Y. H.; Wang, X. G.; Tong, L. *J. Mater. Res.* **2010**, *25*, 1336−1343.
(3) Xi, J. M.; Feng, L.; Jiang, L. *Appl. Phys. Lett.* **2008**, *92*, 0531021-1−0531021-3.

(4) Tuteja, A.; Choi, W. J.; McKinley, G. H.; Cohen, R. E.; Rubner, M. F. *MRS Bull.* **2008**, *33*, 752−758.
(5) Tuteja, A.; Choi, W.; Ma, M. L.; Mabry, J. M.; Mazzella, S. A.; Rutledge, G. C.; McKinley, G. H.; Cohen, R. E. *Science* **2007**, *318*, 1618−1622.
(6) Jung, Y. C.; Bhushan, B. *Langmuir* **2009**, *25*, 14165−14173.
(7) Nguyen, T. P. N.; Brunet, P.; Coffinier, Y.; Boukherroub, R. *Langmuir* **2010**, *26*, 18369−18373.
(8) Meng, H. F.; Wang, S. T.; Xi, J. M.; Tang, Z. Y.; Jiang, L. *J. Phys. Chem. C* **2008**, *112*, 11454−11458.
(9) Xue, Z. X.; Wang, S. T.; Lin, L.; Chen, L.; Liu, M. J.; Feng, L.; Jiang, L. *Adv. Mater.* **2011**, *23*, 4270−4273.
(10) Amantonico, A.; Urban, P. L.; Zenobi, R. *Analyst* **2009**, *134*, 1536−1540.
(11) Darmanin, T.; Guittard, F. *J. Am. Chem. Soc.* **2009**, *131*, 7928−7933.
(12) Leng, B. X.; Shao, Z. Z.; de With, G.; Ming, W. H. *Langmuir* **2009**, *25*, 2456−2460.
(13) Zhu, X. T.; Zhang, Z. Z.; Xu, X. H.; Men, X. H.; Yang, J.; Zhou, X. Y.; Xue, Q. J. *Langmuir* **2011**, *27*, 14508−14513.
(14) Bellanger, H.; Darmanin, T.; de Givenchy, E. T.; Guittard, F. *J. Mater. Chem. A* **2013**, *1*, 2896−2903.
(15) Zhang, J. P.; Seeger, S. *Angew. Chem., Int. Ed.* **2011**, *50*, 6652−6656.
(16) Yang, J.; Zhang, Z. Z.; Xu, X. H.; Men, X. H.; Zhu, X. T.; Zhou, X. Y. *New J. Chem.* **2011**, *35*, 2422−2426.
(17) Zhang, G. W.; Hu, J. W.; Liu, G. J.; Zou, H. L.; Tu, Y. Y.; Li, F.; Hu, S. Y.; Luo, H. S. *J. Mater. Chem. A* **2013**, *1*, 6226−6237.
(18) Tsujii, K.; Yamamoto, T.; Onda, T.; Shibuichi, S. *Angew. Chem., Int. Ed. Engl.* **1997**, *36*, 1011−1012.
(19) Fujii, T.; Sato, H.; Tsuji, E.; Aoki, Y.; Habazaki, H. *J. Phys. Chem. C* **2012**, *116*, 23308−23314.
(20) Campos, R.; Guenthner, A. J.; Haddad, T. S.; Mabry, J. M. *Langmuir* **2011**, *27*, 10206−10215.
(21) Cao, L. L.; Price, T. P.; Weiss, M.; Gao, D. *Langmuir* **2008**, *24*, 1640−1643.
(22) Kang, S. M.; Kim, S. M.; Kim, H. N.; Kwak, M. K.; Tahk, D. H.; Suh, K. Y. *Soft Matter* **2012**, *8*, 8563−8568.
(23) Deng, X.; Mammen, L.; Butt, H. J.; Vollmer, D. *Science* **2012**, *335*, 67−70.
(24) Zhao, H.; Law, K. Y. *Langmuir* **2012**, *28*, 11821−11827.
(25) Zhao, H.; Law, K. Y. *ACS Appl. Mater. Interfaces* **2012**, *4*, 4288−4295.
(26) Susarrey-Arce, A.; Marin, A. G.; Nair, H.; Lefferts, L.; Gardeniers, J. G. E.; Lohse, D.; van Houselt, A. *Soft Matter* **2012**, *8*, 9765−9770.
(27) Pan, S. J.; Kota, A. K.; Mabry, J. M.; Tuteja, A. *J. Am. Chem. Soc.* **2013**, *135*, 578−581.
(28) Wang, J. L.; Raza, A.; Si, Y.; Cui, L. X.; Ge, J. F.; Ding, B.; Yu, J. Y. *Nanoscale* **2012**, *4*, 7549−7556.
(29) Kota, A. K.; Li, Y. X.; Mabry, J. M.; Tuteja, A. *Adv. Mater.* **2012**, *24*, 5838−5843.
(30) Zhu, X. T.; Zhang, Z. Z.; Xu, X. H.; Men, X. H.; Yang, J.; Zhou, X. Y.; Xue, Q. J. *J. Colloid Interface Sci.* **2012**, *367*, 443−449.
(31) Zhang, Z. Z.; Zhu, X. T.; Yang, J.; Xu, X. H.; Men, X. H.; Zhou, X. Y. *Appl. Phys. A: Mater. Sci. Process.* **2012**, *108*, 601−606.
(32) Xue, Z. X.; Liu, M. J.; Jiang, L. *J. Polym. Sci., Part B: Polym. Phys.* **2012**, *50*, 1209−1224.
(33) Stober, W.; Fink, A.; Bohn, E. *J. Colloid Interface Sci.* **1968**, *26*, 62−69.
(34) Xiong, D.; Liu, G. J.; Hong, L. Z.; Duncan, E. J. S. *Chem. Mater.* **2011**, *23*, 4357−4366.
(35) Hsieh, C. T.; Wu, F. L.; Chen, W. Y. *Mater. Chem. Phys.* **2010**, *121*, 14−21.
(36) Yu, H. J.; Luo, Z. H. *J. Polym. Sci., Part B: Polym. Phys.* **2010**, *48*, 5570−5580.
(37) Yu, H. J.; Luo, Z. H. *J. Polym. Sci., Part A: Polym. Chem.* **2011**, *49*, 174−183.
(38) Xiong, D. A.; Liu, G. J.; Duncan, E. J. S.. *ACS Appl. Mater. Interfaces* **2012**, *4*, 2445−2454.
(39) Hao, L. F.; An, Q. F.; Xu, W. *Fiber. Polym.* **2012**, *13*, 1145−1153.
(40) He, G.; Hu, J.; Liu, G.; Li, Y.; Zhang, G.; Liu, F.; Sun, J.; Zou, H.; Tu, Y.; Xiao, D. *ACS Appl. Mater. Interfaces* **2013**, *5*, 2378−2386.
(41) He, G.; Zhang, G.; Hu, J.; Sun, J.; Hu, S.; Li, Y.; Liu, F.; Xiao, D.; Zou, H.; Liu, G. *J. Fluorine Chem.* **2011**, *132*, 562−572.
(42) Mu, B.; Liu, P.; Tang, Z.; Du, P.; Dong, Y. *Nanomed. Nanotech.* **2011**, *7*, 789−796.
(43) Zhou, L.; Yuan, W.; Yuan, J.; Hong, X. *Mater. Lett.* **2008**, *62*, 1372−1375.
(44) Ding, J. F.; Liu, G. J. *Langmuir* **1999**, *15*, 1738−1747.
(45) Kim, J.; Efimenko, K.; Genzer, J.; Carbonell, R. G. *Macromolecules* **2007**, *40*, 588−597.
(46) Huang, C.; Tassone, T.; Woodberry, K.; Sunday, D.; Green, D. L. *Langmuir* **2009**, *25*, 13351−13360.
(47) Ohno, K.; Akashi, T.; Huang, Y.; Tsujii, Y. *Macromolecules* **2010**, *43*, 8805−8812.
(48) Tsujii, Y.; Ohno, K.; Yamamoto, S.; Goto, A.; Fukuda, T. *Adv. Polym. Sci.* **2006**, *197*, 1−45.
(49) Park, J. T.; Seo, J. A.; Ahn, S. H.; Kim, J. H.; Kang, S. W. *J. Ind. Eng. Chem.* **2010**, *16*, 517−522.
(50) Singh, L. P.; Bhattacharyya, S. K.; Mishra, G.; Ahalawat, S. *Appl. Nanosci.* **2011**, *1*, 117−122.
(51) Sun, J. T.; Hong, C. Y.; Pan, C. Y. *J. Phys. Chem. C* **2010**, *114*, 12481−12486.
(52) Mihaly, J.; Sterkel, S.; Ortner, H. M.; Kocsis, L.; Hajba, L.; Furdyga, E.; Mink, J. *Croat. Chem. Acta* **2006**, *79*, 497−501.
(53) Wu, T.; Zhang, Y. F.; Wang, X. F.; Liu, S. Y. *Chem. Mater.* **2008**, *20*, 101−109.
(54) Ajayan, P. M.; Iijima, S. *Philos. Mag. Lett.* **1992**, *65*, 43−48.
(55) Liu, C. H.; Pan, C. Y. *Polym. Chem.* **2011**, *2*, 563−566.
(56) Li, D. J.; Jones, G. L.; Dunlap, J. R.; Hua, F. J.; Zhao, B. *Langmuir* **2006**, *22*, 3344−3351.
(57) Osterholtz, F. D.; Pohl, E. R. *J. Adhes. Sci. Technol.* **1992**, *6*, 127−149.
(58) Xiong, D. A.; Liu, G. J.; Duncan, E. J. S. *Langmuir* **2012**, *28*, 6911−6918.
(59) Salon, M. C. B.; Gerbaud, G.; Abdelmouleh, M.; Bruzzese, C.; Boufi, S.; Belgacem, M. N. *Magn. Reson. Chem.* **2007**, *45*, 473−483.
(60) Kim, S.; Kim, E.; Kim, S.; Kim, W. *J. Colloid Interface Sci.* **2005**, *292*, 93−98.
(61) Volkov, V. V.; Plate, N. A.; Takahara, A.; Kajiyama, T.; Amaya, N.; Murata, Y. *Polymer* **1992**, *33*, 1316−1320.
(62) Wenzel, R. N. *Ind. Eng. Chem.* **1936**, *28*, 988−994.
(63) Cassie, A. B. D.; Baxter, S. *Trans. Faraday Soc.* **1944**, *40*, 0546−0550.
(64) Facio, D. S.; Mosquera, M. J. *ACS Appl. Mater. Interfaces* **2013**, *5*, 7517−7526.